FEDSM-ICNMM2010-31042

APPLICATION OF AN IMMERSED BOUNDARY METHOD TO FLOW IN CEREBRAL ANEURYSMS AND POROUS MEDIA

Julia Mikhal[*]
Multiscale Modeling and Simulation
Department of Applied Mathematics
University of Twente
7500 AE Enschede, The Netherlands
Email: j.mikhal@ewi.utwente.nl

David J. Lopez Penha
Multiscale Modeling and Simulation
Department of Applied Mathematics
University of Twente
7500 AE Enschede, The Netherlands
Email: d.j.lopezpenha@utwente.nl

Steffen Stolz
Philip Morris International R&D
Philip Morris Products S.A.
Quai Jeanrenaud 5
2000 Neuchâtel, Switzerland
Email: steffen.stolz@pmintl.com

Bernard J. Geurts
Multiscale Modeling and Simulation
Department of Applied Mathematics
University of Twente
7500 AE Enschede, The Netherlands
Email: b.j.geurts@utwente.nl

ABSTRACT

We present the development and application of an immersed boundary (IB) method for the simulation of incompressible flow inside and around complex geometrical shapes and cavities. The IB method is based on a volume-penalization method that is applied throughout the domain, rendering the velocity in stationary solid parts negligibly small, while the flow in the open parts of the domain is governed by the Navier-Stokes equations. The flow solver is based on a skew-symmetric finite-volume discretization in combination with explicit time-stepping for the convective and viscous fluxes, and implicit time-stepping for the IB forcing term. The complex geometry is characterized in terms of a so-called 'masking function' which equals unity in the solid parts and zero in the open parts of the domain. The focus is on the accuracy with which gradients of the solution close to solid walls can be approximated using the IB methodology. We investigate this for flow through a model of an aneurysm as may develop in the circle of Willis in a human brain, and to flow in a structured porous medium composed of a regular spatial arrangement of square rods. The shear stress acting on the vessel walls in case of flow through an aneurysm and the permeability of the porous material were analyzed. The computational method converges as a first order method for Poiseuille flow, with a considerable influence derived from the precise definition of the masking function near solid-fluid interfaces. We identify the best masking function strategy and show that for plane Poiseuille flow even second order convergence may be obtained. Qualitatively reliable results are obtained already at modest resolutions of 8-16 grid cells across a characteristic opening in the flow domain, e.g., the vessel diameter or the size of the gap between individual square rods.

INTRODUCTION

The prediction of flow that arises inside and around solid objects with a complex shape is a key application area for immersed boundary (IB) methods [1]. IB methods allow for the computation of flows in complex geometries, e.g., cerebral aneurysms [2] and porous media [3]. For brain aneurysms there is a growing

---

[*]Address all correspondence to this author.

medical need to predict the flow behavior and shear stresses in order to more completely plan and foresee the effect of surgical intervention. These stresses are thought to be related to the likelihood of long-time rupture of aneurysms. Likewise, the computation of transport in porous media is of great importance to process engineering, particularly aimed at (i) a more complete control of the conditions, and (ii) better use of scarce resources.

In this paper we discuss a basic volume-penalization IB method and its application to flow in complex cavities and around a staggered arrangement of square rods. The flow domain is characterized by a so-called 'masking function' in which solid and fluid parts are identified by a value of '1' or '0' respectively. This method of representing a complex shaped domain allows for a range of sources for specifying the geometry. In various technological applications the design of the flow domain is known from its CAD file – this is a very precise source for the specification of the masking function. In certain applications, e.g., when complex porous media are involved, consisting of biomass, it is possible to extract detailed information about the inner structure of a block of porous material using computed tomography imaging. This yields a large number of slices through a porous block, allowing an approximate identification of the fluid and the solid parts. In medical applications the shape of cerebral aneurysms developing in patients can be inferred from three-dimensional rotational angiography. This provides a detailed impression of the complex cavity and vessel structure that may be under risk of rupture.

The accuracy with which the flow field in a complex geometry can be computed on the basis of an IB method depends strongly on the spatial resolution of the smallest details of the domain, as captured by the masking function. As in some cases the domain may not be specified beyond a rather modest spatial resolution, the issue of sensitivity of predictions on the quality of the geometrical characterization is important to include. It is particularly important to assess which conclusions can be reliably drawn from simulations, and what aspects remain unclear because of uncertainties in the actual flow conditions and the geometry. This issue can be addressed in detail using computational modeling.

The convergence of IB-predictions toward the actual solution of the Navier-Stokes equations is a key element that decides about the usefulness of this approach for realistic applications. We analyze this in detail for Poiseuille flow, both in a plane channel and in a cylindrical tube. The precise definition of the masking function in the near-wall region is shown to have a considerable influence on the error-levels that can be attained. For plane Poiseuille flow it is shown that the approximation of the no-slip condition at a solid wall may be implemented such that the accuracy of the overall method is lifted from first to second order. In case of flow in a cylindrical tube the non-alignment of the geometry with the Cartesian grid is shown to imply first order convergence only. Also in this example, the precise definition of

the masking function can strongly reduce the error-level – a definition in which the numerical flow domain is entirely inside the physical flow domain of the problem considered is found to be beneficial for reducing the error levels.

The flexibility of the IB method is illustrated with two applications; one with a biomedical context, concerning flow in a cerebral aneurysm, and one from process engineering, involving the prediction of flow in a porous medium. We adopt an energy-conserving finite-volume discretization that is, by construction, stable on any spatial resolution [4]. In these applications only the masking function needs to be specified properly and the spatial resolution should be fine enough to capture, at least qualitatively, the smallest geometrical details. From the study of Poiseuille flow we infer that about 16 grid points per 'opening' in the flow-domain suffices to obtain reliable predictions. This brings a large range of laminar and transitional flow in realistically complex flow geometries within reach of large-scale computing. In this way, numerical flow simulation in combination with the IB approach can provide reliable information about the inner working of flow equipment that would otherwise not be attainable from physical experimentation. Such computational modeling can help improve process-engineering steps and support surgical interventions in case of medical applications.

The organization of this paper is as follows. We first present a brief sketch of the IB method that is adopted. Then we proceed with a discussion of the convergence of numerical predictions to the exact analytical solution in case of Poiseuille flow. We consider both plane channel flow and flow in a cylindrical tube. The application of the IB method to flow in cerebral aneurysms and flow through structured porous media is included to illustrate the flexibility of the method. Concluding remarks will be gathered in the final section.

IMMERSED BOUNDARY METHOD

In this section we give a brief review of the volume-penalization immersed boundary (IB) method that is considered in this paper. We focus on incompressible fluids whose dynamics are governed by the conservation of mass and momentum:

$$\partial_j u_j = 0, \qquad (1)$$

$$\partial_t u_i + \partial_j (u_j u_i) + \partial_i p - \frac{1}{Re} \partial_{jj} u_i - f_i = 0; \qquad (2)$$

where ∂_t and ∂_j denote partial derivatives with respect to time t and spatial coordinate x_j, u_j denotes the velocity component in the x_j direction and p is the pressure. The Reynolds number $Re = UL/\nu$ is a measure for the relative importance of the nonlinear convective fluxes and the linear viscous fluxes [5]; it is expressed in terms of a reference velocity scale U, a reference length-scale L and the kinematic viscosity $\nu = \mu/\rho$ with molecular viscosity given by μ and the fluid mass-density ρ. The forcing

f_i can be used to represent a variety of physical mechanisms that influence the evolution of the flow. Here, we will use this forcing for another purpose, i.e., to approximate no-slip conditions at solid boundaries that are contained in the domain [1].

The IB method enjoys a growing interest in the field of computational science. It provides a strong alternative to conventional numerical simulation methods in case flow in and around very complex spatial shapes in a flow domain is considered. Conventional methods adhere to computational meshes that are body-fitted – for complex flow domains the gridding of the flow domain becomes very time consuming. The task of generating grids that yield an accurate discrete computational model is correspondingly difficult, up to the point of becoming impractical. Instead, the IB method can be formulated entirely in terms of a uniform Cartesian grid. The geometry over and through which the flow takes place is simply immersed in a 'block' of physical space. These striking differences in the computational strategies also imply important consequences for the accuracy with which flow near solid boundaries may generally be captured. Conventional body-fitted methods allow, in principle, for a precise representation of no-slip conditions at the body. In contrast, the accuracy achieved by an IB method generally suffers from the non-alignment of the interface between solid and fluid regions with the Cartesian grid. This is even more challenging if, next to the flow velocity, information about the gradient of the velocity, or of a passive scalar such as temperature or chemical species, is of interest. For such situations we identify spatial resolution requirements that are needed to yield reliable results.

We employ a basic IB method in which the forcing term f_i represents a volume penalization. The impenetrability of a solid wall to fluid flow is approximated by direct penalization of the flow from entering the solid domain. This is represented here by a forcing term

$$f_i = \frac{1}{\varepsilon}\Gamma(\mathbf{x})u_i(\mathbf{x},t), \tag{3}$$

in which the control parameter $\varepsilon \ll 1$ (a typical value used is $\varepsilon = 10^{-10}$) and $\Gamma(\mathbf{x})$ denotes the so-called 'masking function' or 'phase indicator' which assumes the value '1' in case the point $\mathbf{x}$ belongs to a solid part of the flow domain and '0' in case it is located in an open fluid-filled part of the domain. In this way the entire flow domain Ω is decomposed into a solid part Ω_s and a fluid part Ω_f; while in Ω_f the forcing is absent and the original, incompressible Navier-Stokes equations govern the flow, the various fluxes in the momentum equation are entirely overruled by the IB forcing inside Ω_s. The form of the forcing f_i inside the solid part implies that the velocity components u_i are negligible; if at some location in the solid u_i would, for some reason, have become non-zero then the forcing drives the local velocity back to negligible values. In the region near the interface between the solid and the fluid parts of the domain the velocity field would be forced to negligible values within a very thin strip of the grid. A sufficiently small value of ε will imply a very localized region in which a non-trivial flow in Ω_f connects to a solution with negligible values in Ω_s. This rough sketch identifies that the simple volume forcing (3) can indeed approximate a no-slip boundary condition, localized within the grid-scale.

The equations resulting from the introduction of the forcing (3) in the Navier-Stokes equations need to be treated numerically. We adopt a finite-volume discretization that preserves the skew-symmetry of the nonlinear convective fluxes and the positive-definite dissipative nature of the viscous fluxes [4]. In particular, this method can be shown to be stable on any (coarse) resolution, without having to resort to artificial dissipation that would smear out small-scale details in a numerical solution. This is particularly important in case turbulent flow is simulated with dynamically important fluid motions on a wide spectrum of scales. Also for laminar flows in a complex porous medium the use of such a discretization is important since a wide range of flow-scales can emerge from the passage of a flow through a fine 'maze' of obstructing elements. In order to capture e.g., forces on the solid parts of the domain or heat transfer characteristics from the fluid to the solid, the treatment of the small near-wall flow structures is essential. A second order accurate method for the fluxes is employed, implemented on a staggered grid. The effect of these fluxes is integrated in time using an explicit time-stepping algorithm of Adams-Bashforth type [6]. The contribution of the forcing term $\mathbf{f}$ is integrated implicitly in time, which overcomes severe stability problems that would arise with explicit methods as $\varepsilon \ll 1$.

The staggered grid arrangement poses the particular question how exactly the masking function Γ should be defined. Globally, Γ is easily defined as indicated above. However, there is some freedom in its definition on grid-scale near a solid-fluid interface. In this paper, first, we choose to work with an individual grid cell as the smallest elementary unit; this implies that a grid cell is considered either as part of the solid or as part of the fluid. If the center of the cell is solid or fluid, then we assign this property for the entire grid cell. Second, we need to identify which component of the solution is used as a basis for the masking function. In fact, as all three velocity components u_i and the pressure p are defined on their respective grids, one may consider Γ_{u_i} or Γ_p. Also, combinations of these are possible in principle, e.g., the sum of all velocity-based masking functions. We choose to work with Γ_p in most applications, which defines the precise location (within the resolution of the adopted grid) of the solid-fluid interface in a 'staircase' approximation. Using the inter-relation between Γ_p and Γ_{u_i}, one may readily infer the velocity-based masking functions from the pressure-based representation. The use of Γ_p uniquely defines the geometry of the flow domain and is not biased toward one of the coordinate directions, as would be the case with one of the Γ_{u_i}.

In the next section we will consider the performance of the

IB method in combination with the skew-symmetric discretization and determine the accuracy of predictions in relation to the spatial resolution that is used.

VALIDATION AND CONVERGENCE

The convergence of the volume-penalization IB method is studied on the basis of laminar Poiseuille flow in a straight channel and in a cylindrical tube. This represents a set of test-cases of growing complexity, for which the exact analytical solution is available as point of reference. For the channel flow we will determine the importance of approximating the no-slip condition exactly at the solid wall, or shifted by half a grid cell. The cylindrical tube application tests the IB method for geometries that are not aligned with the Cartesian grid; this test-case will establish that the error-level depends considerably on the precise incorporation of the cylindrical wall.

Plane Poiseuille flow is one of the few exact solutions to the incompressible Navier-Stokes equations [7]. The basic geometry consists of two infinitely extended parallel plates. The flow is in the streamwise x_1 direction, while the wall-normal and spanwise coordinates are denoted by x_2 and x_3 respectively. The parallel plates are located at $x_2 = 0$ and $x_2 = 1$. In a non-dimensional form the velocity profile is given by $u_2 = u_3 = 0$ and

$$u_1(x_2) = 4U_{max}x_2(1 - x_2), \qquad (4)$$

where U_{max} is the maximal velocity in the flow, arising at the center-plane between the two parallel plates. The velocity U_{max} corresponds directly to the external pressure gradient that is imposed to maintain the flow. In case of flow through a cylinder aligned with the x_1 axis, the Poiseuille profile is given by

$$u_1(r) = U_{max}(1 - r^2), \qquad (5)$$

where $0 \leq r \leq 1$ is the radial coordinate. These two parabolic profiles provide strict tests for the IB method; in the following we investigate the achieved accuracy as a function of spatial resolution.

By defining the masking function appropriately, an IB model can be obtained with which the analytical Poiseuille flow can be approximated numerically. We consider the plane Poiseuille flow first. In Fig. 1 we collect predictions of the streamwise velocity profile obtained at a range of resolutions in the wall-normal direction. We illustrate two ways of approximating the no-slip condition at the solid wall. In the first method we assume the solid walls at $x_2 = 0$ and $x_2 = 1$ to coincide with a surface of the pressure control volume – this implies that the condition for the wall-normal component $u_2 = 0$ is imposed exactly at the wall, but that the no-slip approximation for the dominant streamwise
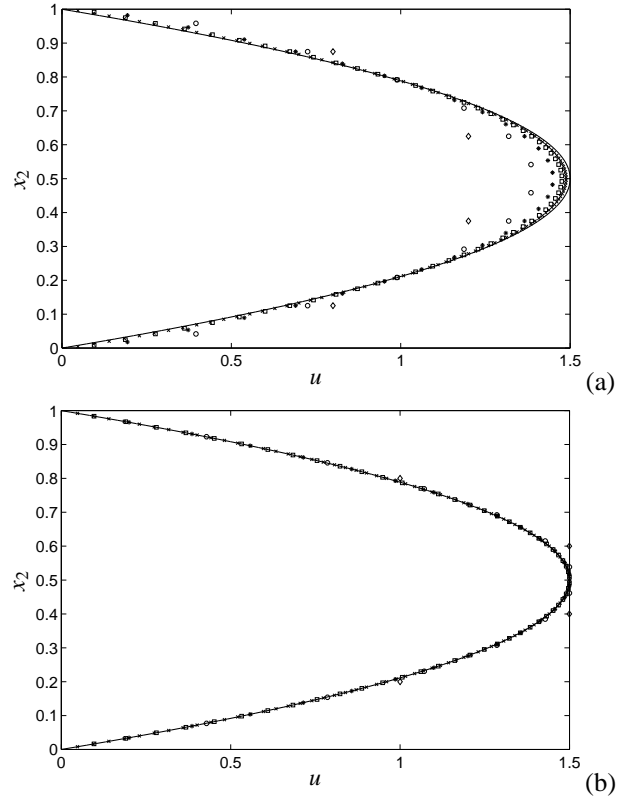

FIGURE 1. Streamwise velocity component $u(x_2)$ at various spatial resolutions n_y and $Re = 1$. In (a) we show the convergence toward the Poiseuille profile in the reference case in which no-slip conditions for the streamwise velocity are imposed at half a grid cell inside the wall, in (b) the no-slip conditions were imposed exactly at the location of the wall. Symbols correspond to the choice of $n_y = 2^k$ with $k = 2, \ldots, 7$.

velocity component is off by half a grid cell. We refer to this as the 'reference' method. In the second method we identify the location of the wall with the center of the pressure control volume. Shifting by half a grid cell we now impose $u_1 = 0$ exactly at the wall and approximate the wall-normal condition with half a grid cell inaccuracy. For both methods of imposing the no-slip boundary condition, we observe a clear convergence of the numerical results toward the analytical solution. On closer inspection it appears that the convergence toward the exact solution is faster with the 'shifted' method, compared to the 'reference' method.

The convergence of the numerical solution toward the exact solution for the plane Poiseuille flow can be quantified in terms of the discrete l^2 or l^∞ (max-) norms. The findings for the two methods of imposing the no-slip boundary conditions in our IB method are collected in Fig. 2. The general impression seen in Fig. 1 is now confirmed. The simulation error on any grid resolution is considerably lowered if the no-slip condition for the dominant streamwise velocity component is imposed exactly at
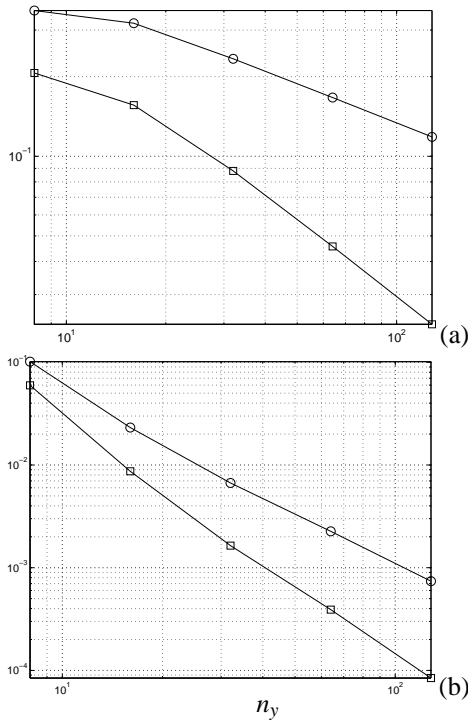
FIGURE 2. Convergence rates of the error between the analytical and the numerical solution in l^∞ (squares) (or max-) norm and l^2-norm (circles) for increasing resolution in the wall-normal direction n_y. The results in (a) correspond to the reference method with no-slip conditions for the streamwise velocity component imposed half a grid cell inside the wall and in (b) the no-slip conditions imposed exactly at the location of the wall.

FIGURE 3. Definition of the 'inner' (a), 'middle' (b) and 'outer' (c) strategy for defining the masking function across a cylindrical tube. Either all four grid points are in the fluid (a), or at least three (b) or at least two (c) to distinguish the different strategies. Grid cells that are identified with the fluid region are drawn in solid lines.

the solid wall, instead of approximately shifted by half a grid cell. In addition to the level of error, we also observe that the rate of convergence increases from first order to second order (in the max-norm) in case the no-slip condition for the streamwise velocity component is imposed exactly at the wall. This property is currently being investigated in more detail in order to develop near-wall treatments that converge as a second order method for general, smooth geometries. This generalized algorithm is considered for skewed and curved geometries and will be published elsewhere.

The convergence of the IB method toward the Poiseuille velocity profile is investigated next for laminar flow in cylindrical tubes. Motivated by the results for the plane channel flow, we identify three methods of identifying the masking function. These are sketched in Fig. 3; we refer to these as 'inner', 'middle' and 'outer', depending on the criterion when exactly a grid cell is counted as part of the *solid* region. In the 'inner' strategy a grid cell is considered part of the fluid region if all four of its corner-points are in the fluid. The 'middle' strategy also includes grid cells that share 3 of its corner points with the fluid and the
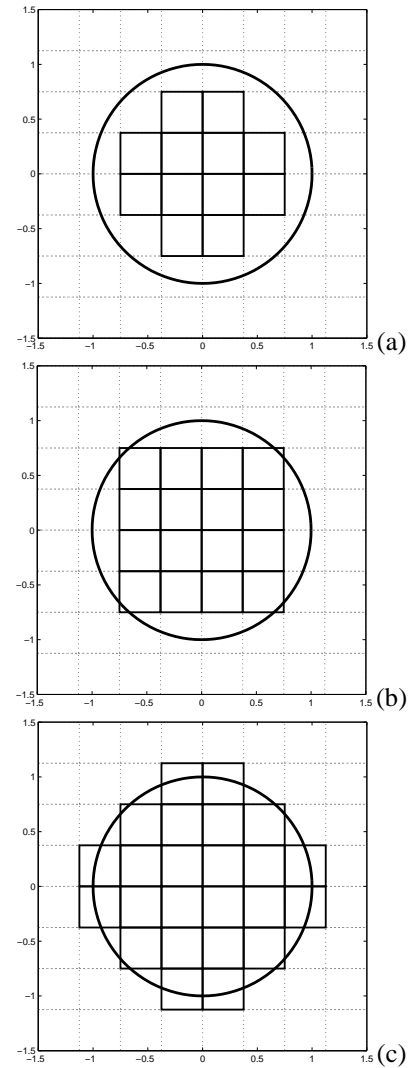
'outer' strategy further allows grid cells with only 2 corner points in the fluid. We performed simulations on a range of grids for this flow problem and investigated the accuracy of predictions for the inner-middle-outer strategies.

The convergence of the numerical results, as measured in the discrete l_∞-norm, is collected in Fig. 4. We observe that all three strategies display first order convergence. This appears consistent with the results obtained for the plane channel flow in case the no-slip condition is imposed within half a grid cell of the solid wall. In case of a cylindrical tube, the non-alignment of the
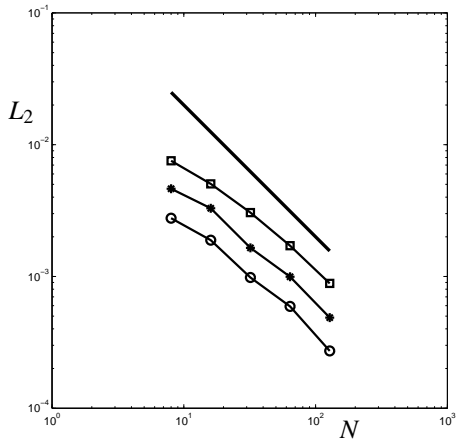
FIGURE 4. Convergence of the discrete l_2-norm of the error in the numerical solution compared to the exact Poiseuille profile as a function of the spatial resolution N. The solid curve denotes first order convergence and the labels are such that 'squares' denote the 'outer', 'asterisks' the 'middle' and 'circles' the 'inner' strategy for the definition of the masking function.

Cartesian grid with the precise geometry implies that the approximate no-slip condition in the IB method is in all points within half a grid cell. We observe a strong dependence of the level of the error on the masking strategy, with a strong improvement in the l_∞-norm if we adopt the 'inner' strategy for defining the fluid part of the domain. If we use a masking function for the fluid region that is entirely inside the cylinder wall, i.e., the fluid domain is 'retracted' by about half a grid cell from the actual location of the cylinder wall, then the predictions at all resolutions are more accurate. This relation between the error-level and the precise definition of the masking function near solid walls will be exploited to achieve higher accuracy in more general geometries – this is a topic of ongoing investigations.

FLOW IN MODEL ANEURYSMS

The application of the IB method to flow inside curved vessels and model aneurysms, as may develop in a human brain, is presented in this section. We consider simple geometrical shapes and investigate the flow field and the corresponding shear stress that arises.

In Fig. 5 we display an impression of the developing flow in a curved cylindrical vessel and in a model aneurysm that contains in addition a spherical cavity. The flow is simulated at a Reynolds number of $Re = 100$, and the unsteady solution is followed time-accurately. The effect of the IB masking function for the solid region is clearly observed in terms of the regions of 'essentially' zero velocity outside the flow domain. The connection with the flow inside the tube appears to be correctly captured – the approximate no-slip condition is expressed in a very narrow strip of
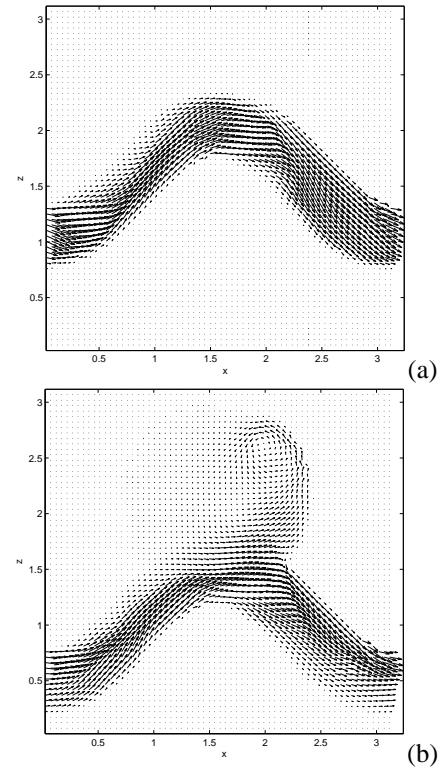

FIGURE 5. Snapshot of the developing flow inside a curved cylindrical tube, without (a) and with (b) a spherical cavity attached. The flow is visualized in a cross-section through the geometry, by plotting the velocity vectors corresponding to the u_1 and u_2 velocity components.

the Cartesian grid, as is desired from the IB volume-penalization method. The addition of a spherical cavity is seen to affect the flow in the curved tube, which leads to the development of a detached 'jet' that proceeds to flow toward the wall of the cavity, producing a vortical structure that fills a large part of the spherical cavity with a detached, recirculating flow. The occurrence of such flow structures contributes to an increase of the average 'residence time' of blood inside the flow domain, expressing a deterioration of the quality of transport of nutrients and waste products to and from the tissue surrounding the aneurysm. This can be an important indicator for the rate at which health risks may develop.

The main challenge for the IB method in case of flow through model aneurysms is in capturing the flow near the boundary; which is required to compute the shear stress. We define the shear stress in terms of the gradient of the velocity. The rate of strain tensor $\boldsymbol{S}$ is such that

$$S_{ij} = \frac{1}{2}\left(\partial_i u_j + \partial_j u_i\right). \tag{6}$$
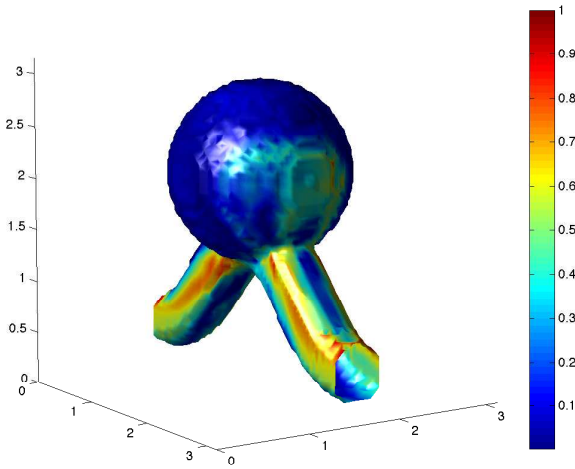
6

FIGURE 6. Predicted shear-stress distribution over the vessel wall of a model aneurysm, composed of a curved cylindrical tube onto which a spherical cavity is attached. The unsteady flow that develops at $Re = 100$ is simulated time-accurately and a characteristic impression of the shear stress is shown. The spatial resolution is $64 \times 64 \times 64$.

The shear stress ξ is a measure for the off-diagonal components of $\mathbf{S}$. We introduce $\Xi_{ij} = S_{ij}$ if $i \neq j$ and $\Xi_{ii} = 0$. Then,

$$\xi^2 = \Xi_{ij}\Xi_{ij} = \boldsymbol{\Xi} : \boldsymbol{\Xi}. \tag{7}$$

The distribution of the shear stress ξ across the vessel wall is an important indicator for the forces that act on the wall. This makes the shear stress a key quantity of relevance for the prediction of long-term risk of rupture of the aneurysm wall. In Fig. 6 the normalized shear-stress distribution is shown at a characteristic stage in the development of the flow. We observe that the detached jet that was discussed above, impinges on the wall of the spherical model aneurysm and creates a region of intensified shear stress. The shear-stress ξ is also quite large in the curved cylindrical tube that is connected to the sphere. The IB method appears to provide a reliable impression of the distribution of the shear stress, showing the flexibility of the approach. A detailed analysis of the accuracy with which ξ is predicted requires a full grid-refinement study, which will be the subject of an upcoming publication.

FLOW IN STRUCTURED POROUS MEDIA

Laminar flow in a complex porous medium can be simulated in full detail using the IB method. We consider configurations that are composed of square rods placed in periodic arrangements. We show the flexibility of the IB method in dealing with such flow problems and quantify the overall permeability that is obtained at a range of Reynolds numbers.
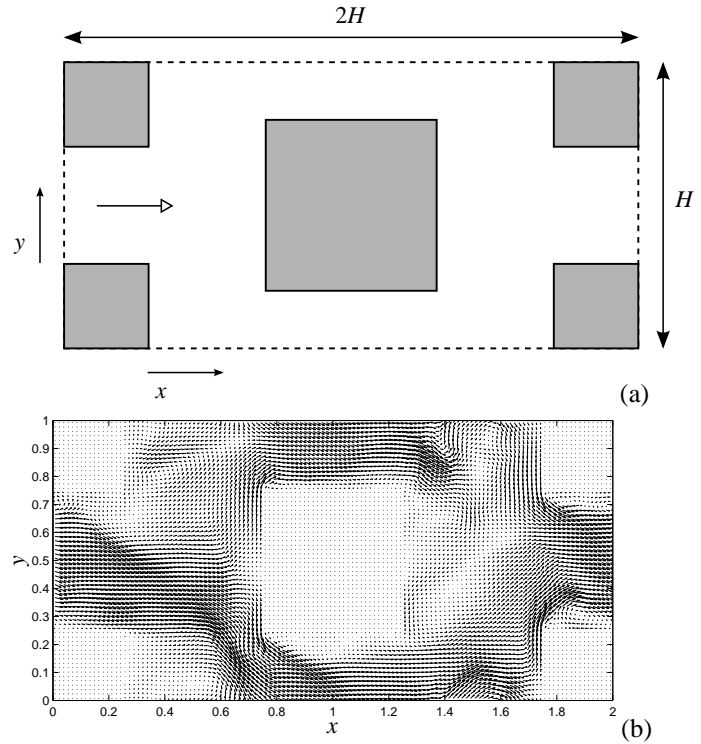

FIGURE 7. In (a) we define a periodic unit of a staggered arrangement of square rods. In (b) a snapshot of the developing flow in this structured porous medium is shown, simulated at $Re = 600$. The spatial resolution in the plane shown is 128×64.

For porous media simulations, the intricate geometry of the medium requires an IB approach to compute local velocity and pressure. In Fig. 7(a) we show the definition of the flow domain in terms of the periodic unit in which the square rods are arranged. Only a two-dimensional cross-section is shown; the full geometry is treated in three spatial dimensions. In this geometry the IB method can readily yield an impression of the developing flow as shown in Fig. 7(b). At a Reynolds number of $Re = 600$ (based on the volume-average velocity $|\langle \mathbf{u} \rangle|$ and the height H) we observe that a rather intricate pattern of vortical flow structures emerges, that appears to be well captured by the current IB method, based on the pressure-based masking function, i.e., the reference method.

Various macroscopic properties of the flow through a structured porous medium can be extracted on the basis of the available microscopic flow predictions. As an illustration, we consider the large-scale permeability of this model porous medium at various Reynolds numbers. In Fig. 8 we show the macroscopic pressure gradient that develops across a periodic unit when a flow is maintained in the x_1-direction. We compare simulation results obtained at two spatial resolutions. The agreement illustrates
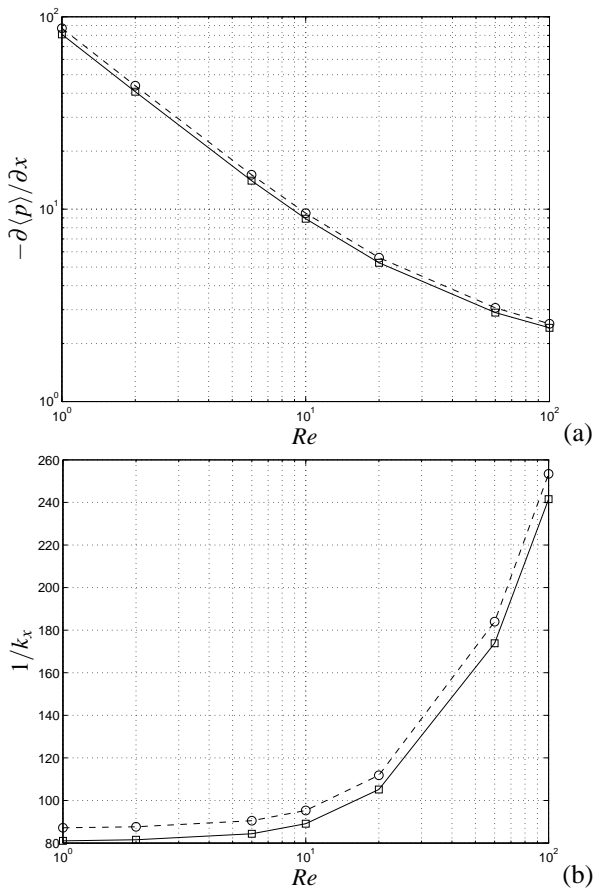
7

FIGURE 8. Dimensionless macroscopic pressure gradient in the x_1-direction as a function of the Reynolds number (a) and the corresponding permeability in the x_1-direction (b). The dashed line represents numerical simulation results at a resolution of 64×64 (marked with squares) and 128×128 (marked with circles).

the accuracy of the simulations in case of slow flow, i.e., low Reynolds numbers. For a related 'in-lined' arrangement [8, 9] the computed macroscopic pressure gradient was compared to the Darcy-Forchheimer expression, showing a close agreement.

CONCLUDING REMARKS

We discussed the development and grid-convergence of a volume-penalizing immersed boundary method, applied to complex flow domains motivated by cerebral aneurysms and arrangements that model a structured porous medium. The focus was on the accuracy with which flow near a solid boundary can be simulated, e.g., in view of the desire to predict shear-stresses at the wall of blood vessels. It was shown that the definition of the masking function can have a large influence on the level of the simulation error, and even on the order of accuracy of the overall

method, in case of plane channel flow. This aspect will be utilized in the future to achieve higher order convergence for more general, smooth flow domains. Moreover, we aim to explicitly incorporate physical conservation principles into the near-wall treatment in the computational model and investigate which of these properties is most decisive for the quality of the results.

The application of the IB approach to model aneurysms and flow through a structured porous medium illustrates the flexibility of this IB method in handling flow through very complex flow domains. At modest Reynolds numbers, as considered in this paper, the relatively coarse representation of the solid-fluid interface was shown not to negatively affect the flow prediction too strongly near a solid wall. In future extensions we plan to incorporate flow-structure interactions for cerebral aneurysms, to study pulsatile flow in flexible geometries. This implies the use of a time-dependent masking function with its own dynamics in which material properties of the brain tissue surrounding the vessel structures needs to be incorporated. Flow through a structured porous medium will be extended to incorporate heat and mass transfer, fully coupled to the gas-flow through the fluid domain. In all these extensions the accuracy of the solution, and its spatial derivatives, near the solid-fluid interface are key elements. The freedom in the detailed definition of the masking function near a wall will be exploited to enhance the accuracy of predictions.

REFERENCES

[1] Mittal, R., and Iaccarino, G., Immersed boundary methods, *Annu. Rev. Fluid Mech.*, **37**, 239–261 (2005).

[2] Ferguson, G.G., Turbulence in human intracranial saccular aneurysms, *J. Neurosurg.*, **33**, 485–497 (1970).

[3] Ingham, D.B., and Pop, I., (editors), Transport phenomena in porous media, *Pergamon Press*, (1998).

[4] Verstappen, R.W.C.P., and Veldman, A.E.P., Symmetry-preserving discretization of turbulent flow, *J. Comput. Phys.*, **187**, 343–368 (2003).

[5] Batchelor, G.K., An introduction to fluid dynamics, *Cambridge University Press*, (2000).

[6] Geurts, B.J., Elements of direct and large-eddy simulation, *Edwards Publishing*, (2003).

[7] Young, D.F., Munson, B.R., Okiishi, T.H., and Huebsch, W.W., A brief introduction to Fluid Mechanics, 4th edition, *John Wiley & Sons Inc.*, (1997).

[8] Nakayama, A., Kuwahara, F., Umemoto, T., and Hayashi, T., Heat and fluid flow within an anisotropic porous medium, *J. Heat Transfer*, **124**, 746–753 (2002).

[9] Lopez Penha, D.J., Ghazaryan, L., Geurts, B.J., Stolz, S., and Nordlund, M., An immersed boundary method for computing heat and fluid flow in porous media, *European Conference on Computational Fluid Dynamics*, EC-COMAS CFD 2010, J. C. F. Pereira and A. Sequeira (Eds.), Lisabon, Portugal, (2010).